Published online 26 July 2018

Nucleic Acids Research, 2018, Vol. 46, No. 16 ***8357–8370***
doi: 10.1093/nar/gky655

The signature motif of the *Saccharomyces cerevisiae* Pif1 DNA helicase is essential *in vivo* for mitochondrial and nuclear functions and *in vitro* for ATPase activity

Carly L. Geronimo[1], Saurabh P. Singh[2], Roberto Galletto[2,*] and Virginia A. Zakian[1,*]

[1]Department of Molecular Biology, Princeton University, Princeton, NJ 08544-1014, USA and [2]Department of Biochemistry and Molecular Biophysics, Washington University School of Medicine, Saint Louis, MO 63110, USA

Received February 27, 2018; Revised June 18, 2018; Editorial Decision July 07, 2018; Accepted July 13, 2018

ABSTRACT

Pif1 family DNA helicases are conserved from bacteria to humans and have critical and diverse functions *in vivo* that promote genome integrity. Pif1 family helicases share a 23 amino acid region, called the Pif1 signature motif (SM) that is unique to this family. To determine the importance of the SM, we did mutational and functional analysis of the SM from the *Saccharomyces cerevisiae* Pif1 (ScPif1). The mutations deleted portions of the SM, made one or multiple single amino acid changes in the SM, replaced the SM with its counterpart from a bacterial Pif1 family helicase and substituted an α-helical domain from another helicase for the part of the SM that forms an α helix. Mutants were tested for maintenance of mitochondrial DNA, inhibition of telomerase at telomeres and double strand breaks, and promotion of Okazaki fragment maturation. Although certain single amino acid changes in the SM can be tolerated, the presence and sequence of the ScPif1 SM were essential for all tested *in vivo* functions. Consistent with the *in vivo* analyses, *in vitro* studies showed that the presence and sequence of the ScPif1 SM were critical for ATPase activity but not substrate binding.

INTRODUCTION

RNA and DNA helicases are proteins that perform key functions in all aspects of nucleic acid biology. Bacteria and eukaryotes express multiple helicases, often with non-overlapping functions. For example, *Saccharomyces cerevisiae* encodes 134 proteins (1) with the sequence motifs of helicases. Helicases were first defined by their ability to use the energy of nucleoside triphosphate (NTP) hydrolysis to catalyze the unwinding of duplex nucleic acids, but it is now realized that helicases can have more diverse activities, such as translocation on single-stranded RNA or DNA and protein displacement from a nucleic acid substrate (2).

Based on amino acid sequence similarity, helicases are divided into six superfamilies (SF1–6) (3). SF1 helicases have a conserved helicase core region consisting of two RecA-like domains (4) and seven helicase motifs (I, Ia, II, III, IV, V and VI) (5). The distance between the motifs is also conserved, although the sequences of these spacers are not (6). Furthermore, each superfamily can be divided into multiple smaller helicase families, named for its first identified member. Helicases in the same family have higher sequence similarity within their helicase motifs and sometimes within the spacer regions between the motifs than they do with helicases in a different family. Pif1-like helicases comprise one of the three families of SF1 helicases (7).

A search of the NCBI protein database (https://www.ncbi.nlm.nih.gov/protein) indicates that Pif1 family helicases are found in virtually all eukaryotes, many eubacteria, and some archaea bacteria (8). Most eukaryotes encode a single Pif1 family helicase (e.g. humans and *Schizosaccharomyces pombe*) while some single-celled organisms (e.g. *S. cerevisiae*, *Candida albicans* and *Cryptococcus neoformans*) encode two and a few organisms (e.g. *Trypanosoma brucei* and *Arabidopsis thaliana*) contain even more, and in these cases some of the sequences are quite divergent (8). The other Pif1 helicase in budding yeast, Rrm3, promotes replication past stable protein complexes at over 1000 genomic sites (9), restricts DNA synthesis during replication stress via its Orc5-binding domain (10) and is important for the repair of replication generated double-strand breaks (DSBs) (11).

Saccharomyces cerevisiae Pif1 (ScPif1), the prototypical and best-studied helicase in the Pif1 family, has multiple and diverse *in vivo* functions (Figure 1) [reviewed in (8,12,13)]. ScPif1 was discovered in a screen for genes affecting mitochondrial DNA (mtDNA) recombination (14) and is also critical for the maintenance of mtDNA (15). ScPif1 was rediscovered in a screen for genes affecting telomeres when it was identified as an inhibitor of telomerase-mediated telom-

*To whom correspondence should be addressed. Tel: +1 609 258 6770; Fax: +1 609 258 3980; Email: vzakian@princeton.edu
Correspondence may also be addressed to Roberto Galletto. Tel: +1 314 362 4368; Fax: +1 314 362 7183; Email: galletto@wustl.edu

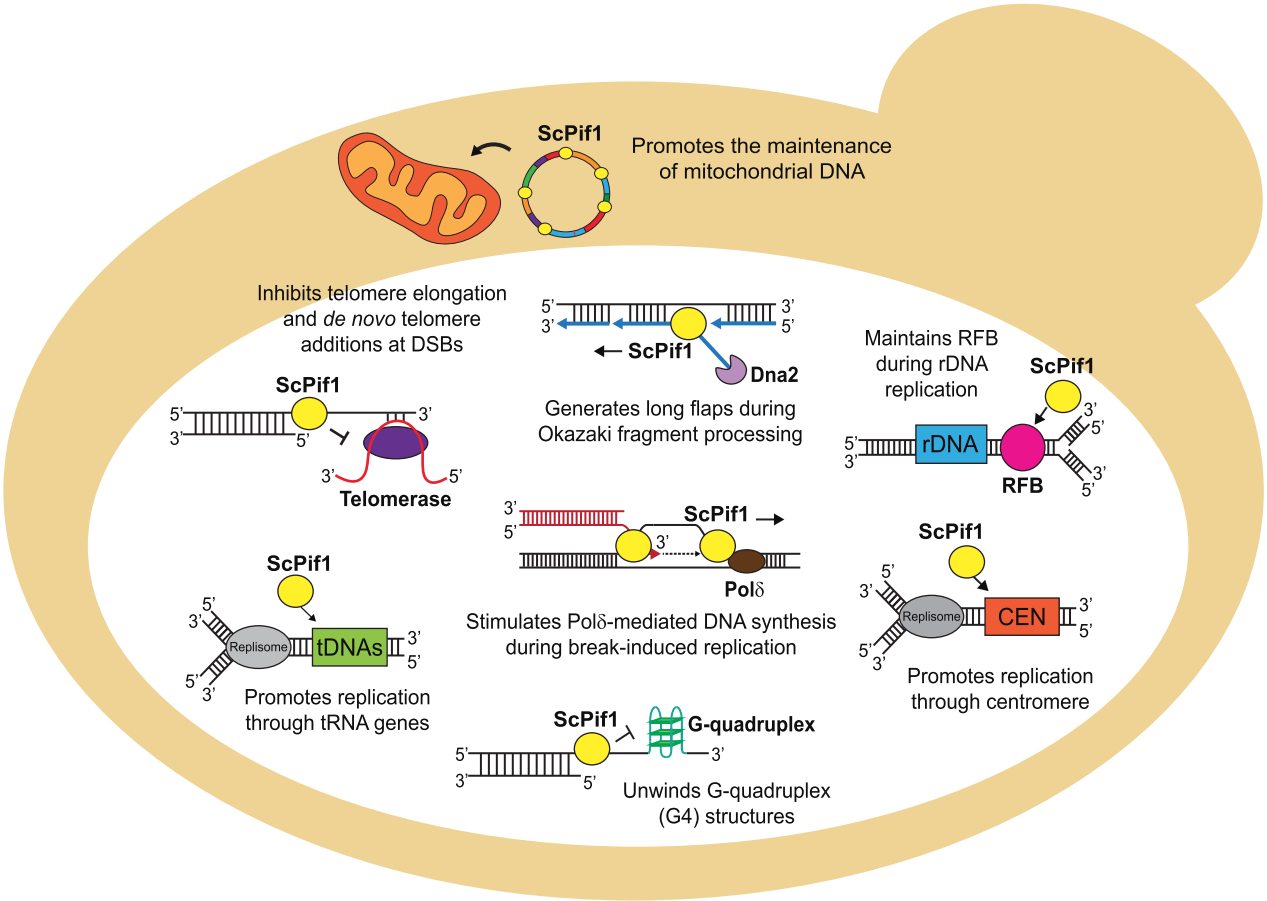

Figure 1. Diagram showing the diverse *in vivo* functions of the ScPif1 DNA helicase. Figure is inspired by an earlier depiction of ScPif1 functions (12). See introduction for references for these functions.

ere lengthening (16,17). ScPif1 inhibits telomerase processivity at both telomeres and DSBs by removing the enzyme from DNA ends (18,19). Its actions at DSBs is regulated by Mec1-dependent phosphorylation (20). When ScPif1 is unable to remove telomerase from DSBs, the rate of gross chromosomal rearrangements (GCRs) dramatically increases due to the formation of terminal deletions (21).

ScPif1's nuclear functions are not limited to telomeres. ScPif1 contributes to semi-conservative DNA replication in multiple ways. It affects Okazaki fragment maturation by generating long flaps that are cleaved by the nuclease activity of Dna2 (22,23). It promotes fork progression and suppresses DNA damage at several hard to replicate sites, such as tRNA genes (24,25), G-quadruplex (G4) structures (26,27), and centromeres (Chen *et al.*, in preparation). In contrast, ScPif1 inhibits fork progression at the replication fork barrier within ribosomal DNA (rDNA), which ensures that replication and transcription occur in the same direction through rDNA repeats (28). ScPif1 stimulates Pol δ-mediated DNA synthesis and bubble migration during break-induced replication repair of DSBs (29,30). ScPif1 also has multiple *in vitro* activities. ScPif1 exhibits weak unwinding activity on conventional 5′-tailed duplex DNA, but robustly unwinds forked DNA (31), G4 structures (26,32,33) and RNA/DNA hybrids (R-loops) (33–35). ScPif1 also displaces proteins from single-stranded DNA (ssDNA) (36), enhances the processivity of DNA polymerase δ (29,37) and promotes annealing of complementary DNA single strands (38). In most cases, it is not clear which of its *in vitro* activities is responsible for a specific *in vivo* function.

At the structural level, most Pif1 family helicases have three regions: an amino terminus, the ∼400–500 amino acid helicase domain and a carboxyl terminus (Figure 2A). While the helicase core is highly conserved, the amino and carboxyl termini diverge both in size and sequence among Pif1 family members. In addition to the seven helicase motifs, the Pif1 helicase domain contains three motifs (A, B and C) whose functions are unknown which are shared with the *Escherichia coli* RecD helicase (39,40). Pif1 family helicases also contain the Pif1 signature motif (SM) that is located between motifs II and III (Figure 2A) (8). In our original description of the SM, we said that it was 21 amino acids in length and was absent from plant Pif1 family helicases (8). As more Pif1 family helicases were sequenced, it became clear that the SM is probably better defined as being 23 amino acids in length, as the next two amino acids are also highly conserved (LI or LV) (Figure 2B). Also at least some plant Pif1 family helicases have the SM, although they tend to be more divergent than those in yeasts and multicellular organisms (C. L. Geronimo, personal observation).

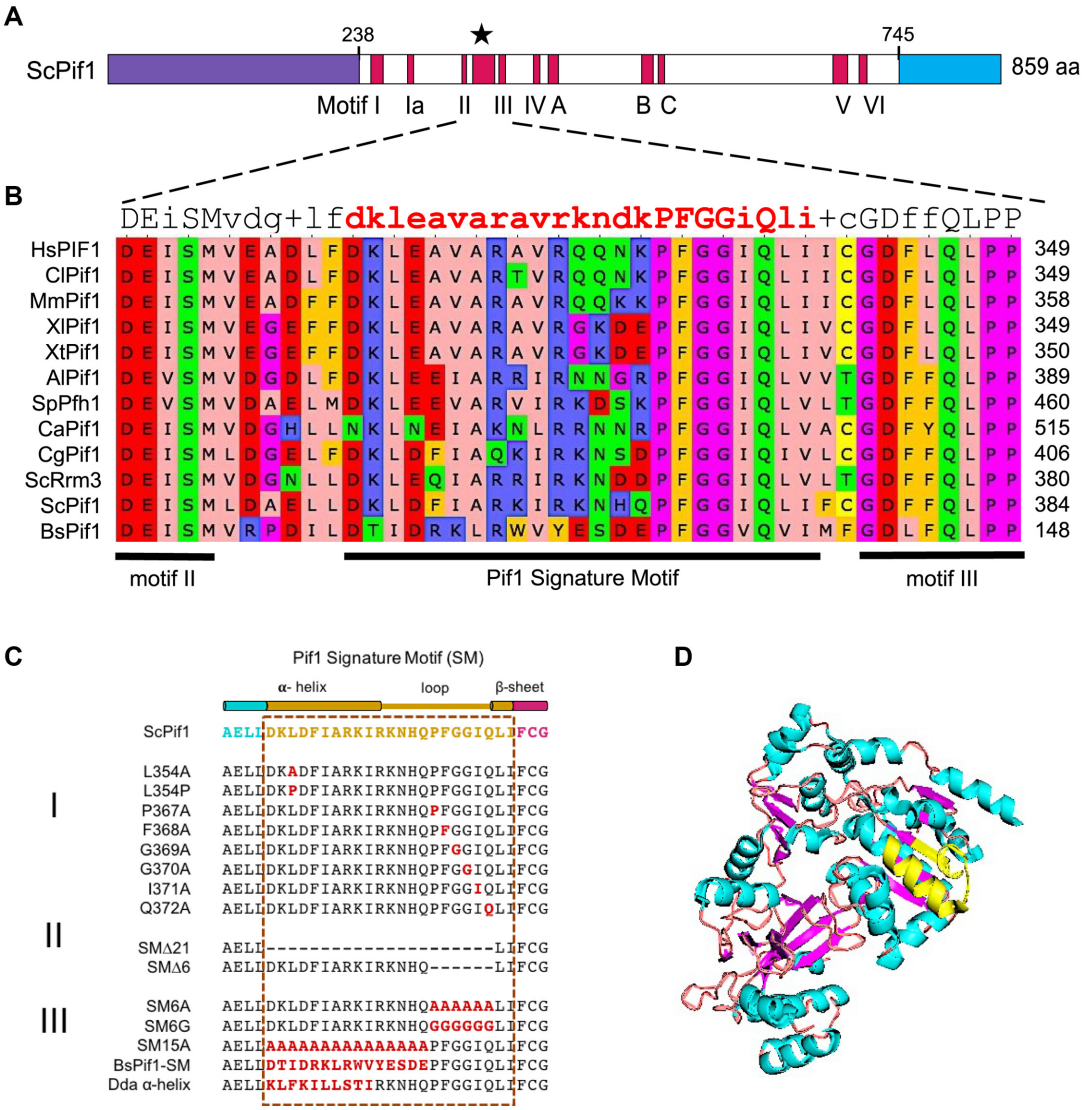

Figure 2. (**A**) Schematic of domains of the ScPif1 DNA helicase. The helicase core domain is in white. The red bars within the core domain are the conserved helicase motifs, and the star indicates the position of the Pif1-family Signature Motif (SM), which is located between helicase motifs II and III. The purple and blue domains are the amino and carboxyl regions of ScPif1, respectively, which vary in size and sequence among different Pif1 family helicases. As indicated, the amino terminus of ScPif1 is 237 amino acids, the helix domain is 508 amino acids and the carboxyl region is 114 amino acids. (**B**) Sequence alignment of Pif1-family SM from different organisms (Al, *Aspergillus lentulus*; Bs; *Bacteroides spp*; Ca, *Candida albicans*; Cg, *Candida glabrata*; Cl, *Canus lupus familiaris*; Hs, *Homo sapiens*; Mm, *Mus musculus*; Sc, *Saccharomyces cerevisiae*; Sp, *Schizosaccharomyces pombe*; Xl, *Xenopus laevis*; Xt, *Xenopus tropicalis*). Protein sequences were obtained from NCBI (https://www.ncbi.nlm.nih.gov), aligned using Clustal Omega and analyzed using Unipro UGENE. The consensus row at the top indicates the most conserved residue at each position or shows a '+' when two or more residues are equally abundant. Residues are colored in accordance to their physiochemical properties: aliphatic/hydrophobic (pink), aromatic (orange), positive charge (blue), negative charge (red), hydrophilic (green), proline/glycine (magenta) and cysteine (yellow). (**C**) SM mutations in ScPif1 generated and analyzed in this study. Mutations include alanine substitutions of conserved residues (I), large and small deletions that are represented by dashed lines (II), and successive amino acid substitutions (III). (**D**) Structure of a truncated ScPif1 helicase (PDB ID: 5O6D, amino acids 237–780) (43) rendered and modified using Pymol (55). Secondary structures are colored as follows: helix (teal), loop (beige) and sheet (pink). The ScPif1 SM, which is shown in yellow, forms an α-helix with an extended loop.

The goal of this study is to determine the functional importance of the SM in Pif1 family helicases, using the budding yeast ScPif1 as a model. Our analysis was informed by the crystal structures of bacterial helicases *Bacteroides sp 3-1-23* (BsPif1) (41) and *Bacteroides sp 2-1-16* (BaPif1) (42) and the helicase domains of the human Pif1 (hPIF1, amino acids 200–641) and ScPif1 (amino acids 237–780) (43). The structures in these papers show that the Pif1 SM folds into an α-helix with an extended loop (41–43). Specifically, the first 10 amino acids (AELL**DKLDFIARKI**) of the SM are part of the α-helix (SM residues are in bold and underlined). The next 11 amino acids of the SM form the extended loop with a turn (RKNHQ**P**FGGIQ) (Pro367 in bold represents the first residue in the turn), and the last two amino acids (L373 and I374) in the SM are part of an adjacent β-sheet structure. The SM of BaPif1 is suggested to stabilize the conformation of regions involved in ssDNA-binding (42). Although a leucine to proline mutation in the

SM of the hPIF1 helicase (hPIF1-*L319P*) is associated with an increased risk of breast cancer (44), the contribution of the SM to specific *in vivo* functions of a Pif1 family helicase has not yet been addressed. By conducting a systematic mutational and functional analysis of the ScPif1 SM, we show that its presence was critical for all tested *in vivo* functions of ScPif1. Moreover, the SM was essential for ATPase activity *in vitro* but not for binding to ssDNA. Our *in vivo* analysis is consistent with *in vitro* studies in an accompanying paper which shows that the SM in the *S. pombe* Pif1 helicase is critical for most of its diverse *in vitro* activities (45).

MATERIALS AND METHODS

S. cerevisiae strains and growth conditions

Unless otherwise indicated, strains were derived from W303 (see Supplementary Table S1 for strains and Supplementary Table S2 for plasmids used herein). To create deletion strains, polymerase chain reaction amplification of selective markers and flanking DNA followed by homologous recombination into the gene of interest was used: *PIF1* was deleted with NatMX6 or His3MX6 and *DNA2* was deleted with KanMX6. The strain for the GCR (MBY77) assay was derived from YPH500. To generate MBY77, *HTX13* on Chr V-L was replaced with the *Kluyveromyces lactis URA3* gene (32). Mutant alleles of *PIF1* were marked with *TRP1* and introduced on the circular centromere plasmid pCG17 via lithium acetate transformation (100 ng of plasmid DNA unless specified otherwise) (46). Depending on the experiment, cells were grown in rich medium YPD (1% yeast extract, 2% peptone and 2% glucose) or synthetic drop-out medium lacking tryptophan (SD–TRP).

Construction of plasmid-borne Pif1 mutant alleles

The *PIF1* promoter was excised from plasmid pVS102 (16) by digestion with PspXI and AgeI (New England Biolabs, NEB) and then cloned into plasmid pMB282 (CEN ARS *TRP1)* containing *PIF1* with a C-terminal 3xFLAG tag (32). The resulting plasmid referred to as pCG17 was verified by restriction enzyme digestion and DNA sequencing and used as the target plasmid for mutagenesis. Mutations within the conserved Pif1-family SM were generated in pCG17 using QuikChange Lightning Site-directed Mutagenesis (Agilent Technologies), Q5® Site-directed Mutagenesis (NEB) or cloned in using gBlocks® gene fragments (Integrated DNA Technologies) and the Gibson Assembly® method (NEB). Mutations were verified by NotI and AvaI restriction enzyme digestion (NEB) and DNA sequencing. The SM mutations analyzed in this study are listed in Figure 2C.

Immunoblot analysis

Yeast total protein extracts were prepared using NaOH precipitation (47). Briefly, 1 ml of mid-log phase cells were pelleted, resuspended in 200 μl of 0.1 M NaOH, incubated at room temperature for 10 min, pelleted, resuspended in 60 μl of sample buffer (2X Laemmli buffer with 1M DTT), boiled for 5 min and pelleted again. At least 10 μl of the supernatant was loaded and the proteins were separated on a 5% (37.5:1 polyacrylamide:bis-acrylamide) sodium dodecyl sulphate-polyacrylamide gel electrophoresis (SDS-PAGE). The proteins were transferred to a nitrocellulose membrane (GE Healthcare) at 4°C and blocked with 5% non-fat dried milk (Lab Scientific) diluted in Tris-Buffer Saline Tween-20. Detection of FLAG-tagged Pif1 proteins was done using mouse monoclonal anti-FLAG M2 primary antibody (Sigma-Aldrich, 1:1000 dilution) and visualized with horseradish peroxidase-conjugated anti-mouse secondary antibody (Bio-Rad, 1:3000 dilution) and ECL detection kit reagents (GE Healthcare).

Telomere blot analysis

Plasmid pCG17 containing wild-type (WT) or Pif1 mutant alleles or an empty vector control (pMB13) was transformed into a heterozygous *PIF1/pif1Δ DNA2/dna2Δ* diploid W303 strain. After sporulation and tetrad dissection, spores were genotyped and haploid *DNA2+ pif1::NatMX6* spores carrying the plasmids were selected by their $KanMX^S$ $NatMX^R$ Trp^+ phenotype. Genomic DNA was extracted from at least three independent transformants (biological replicates) using MasterPure Yeast DNA Purification kit (Epicentre) ∼100 generations after sporulation. Genomic DNAs were digested with XhoI restriction enzyme (NEB), separated by 1% (w/v) agarose gel electrophoresis in Tris-borate ethylenediaminetetraacetic acid (EDTA) and then transferred to a nylon membrane (GE Healthcare). Telomeres were hybridized with α-^{32}P-labeled Y'-sub-telomeric probe (48), imaged on a Typhoon FLA 9500 Phosphorimager system (GE Healthcare) and quantified using ImageQuant TL software (GE Healthcare).

Assay for mitochondrial function

To assay for mitochondrial function, *pif1Δ* cells carrying plasmid pCG17 bearing either a WT or mutant allele of *PIF1* were grown to saturation in 5 ml cultures of SD–TRP medium. From each culture 1 ml of two OD_{660} yeast cells were pelleted, resuspended in sterile water, and 5 μl of 10-fold serial dilutions were spotted onto SD–TRP medium containing 2% glucose or 3% glycerol and grown at 30°C for at least 3 days.

Suppression of *dna2Δ* lethality

Haploid *pif1Δ dna2Δ* cells were generated from a doubly heterozygous (*PIF1/pif1Δ DNA2/dna2Δ*) diploid strain. Using 500 ng pCG17 DNA, Pif1 mutant alleles were transformed into the *pif1Δ dna2Δ* haploid, plated onto YPD and SD–TRP medium and allowed to grow at 30°C for 3–4 days. Growth on SD–TRP medium indicated that the Pif1 mutant was a null allele in this assay, as it suppressed the *dna2Δ* lethality. Cells were also plated on YPD to monitor viable cells.

GCR assay

WT or Pif1 mutant alleles were transformed into MBY77 *pif1::His3MX6*. The GCR assay was performed as previously described (49). Briefly, three to five 5 ml cultures were

grown to saturation in SD–TRP medium at 30°C for 72 h. From each culture 100 μl of diluted (10^{-6}) cells were plated onto non-selective medium (SD–TRP), and the plates were incubated at room temperature for 4 days. In addition, 2 ml of cells were pelleted, resuspended in 300 μl of sterile water, plated onto selective medium supplemented with 5-FOA and canavanine sulfate (SD–TRP+FOA+CAN), and the plates were incubated at 30°C for 4–5 days. GCR rates were calculated using the **F**luctuation **A**nal**y**sis Calculat**or** (FALCOR) web server and the MMS maximum likelihood method (50).

Purification of ScPif1 mutant variants

Pif1 variants harboring mutations or deletions within the 23 amino acid SM were generated with standard site-directed mutagenesis protocols. Preliminary expression tests of ScPif1 variants from a pET28b plasmid indicated that large changes within the SM lead to either low expression or poorly soluble proteins. Therefore, ScPif1 and its mutant variants with a His_6-tag (N- or C-terminal) were re-cloned into a modified pGEX-6p plasmid into which was introduced a NcoI restriction site after a prescission protease site. After induction with 0.7 mM Isopropyl β-D-1-thiogalactopyranoside (IPTG), Rosetta2 (DE3) pLysS cells were grown overnight at 16°C. Cells were opened in Buffer L (20 mM sodium phosphate buffer, pH 7.4, 600 mM NaCl, 20% glycerol, 1 mM EDTA, 0.5 mM Phenylmethyl sulfonyl fluoride (PMSF) and 1 mM Dithiothreitol (DTT)) and the clarified supernatant incubated with glutathione Sepharose™ 4 Fast Flow (GE Healthcare). Following a high salt wash, the bound proteins were eluted with 25 mM glutathione. After cleavage of the GST-tag during dialysis, the proteins were further purified with anion exchange (HighQ, BioRad), cation exchange (HighS, BioRad) and finally eluted from Ni-NTA (Qiagen), as described previously (51). A ScPif1 construct missing the first 237 amino acids and their variants where the ^{367}PFGGIQ^{372} motif was substituted for six glycines was overexpressed from a pET28b plasmid and purified as described (51). ScPif1 and its purified mutant variants were quantified spectrophotometrically (51,52); the concentrations of the mutant variants contaminated with the faster migrating band were quantified by gel densitometry using Pif1 WT as a standard.

ATPase and DNA binding assays

The DNA-dependent ATPase activity of ScPif1 and its mutant variants were determined spectrophotometrically using a β-Nicotinamide adenine dinucleotide reduced disodium salt hydrate (NADH) enzyme-coupled assay as previously reported (51,52). ATPase activity was measured at 30°C in Buffer A (10 mM Hepes (pH 7.4), 100 mM NaCl, 8 mM Mg-acetate and 1 mM DTT) as a function of the concentration of ssDNA (dT_{60}) and at a constant concentration of 1 mM ATP. The data were fitted with the equation $v = k'_{cat}$ [DNA]/(K'_{DNA} + [DNA]). DNA binding was measured in Buffer B (50 mM Tris–HCl (pH 8.1), 100 mM NaCl, 1 mM Mg-acetate and 1 mM DTT) by monitoring the fluorescence quenching of a forked-DNA substrate labeled with 6-carboxy fluorescein. DNA binding isotherms were analyzed with a 1:1 binding model, as described in (52). Standard deviations are from three to four independent experiments.

RESULTS

Experimental strategy to determine the *in vivo* functions of the ScPif1 signature motif (SM)

The SM was identified during sequence alignments of Pif1 proteins as a 21 amino acid stretch that is unique to Pif1 family helicases. When the SM consensus sequence (DKLeXvARaiRKqXkPFGGIQ) was used in a BLAST search, only Pif1 homologues were identified (8). As more Pif1 family helicases were sequenced, it became clear that the SM is probably better defined as being 23 amino acids in length, as the next two amino acids are also highly conserved (LI or LV) (Figure 2B). Although we originally thought the SM was not present in plant Pif1 family helicases, at least some of the plant Pif1 helicases (e.g. *Capsella rubella* and *Trifolium pratense*) have this motif, although they are often more divergent than those in yeasts and multi-cellular organisms (C. L. Geronimo, personal observation).

To determine the function of the SM, we designed a series of mutations within the SM, introduced the mutant genes on centromere plasmids into *pif1Δ* cells and determined the ability of each mutant gene to supply individual Pif1 functions. Our choice of mutations was based in part on structural studies of bacterial and hPIF1 helicases (see 'Introduction'). As a control, we used the *Sc-pif1-K264A* allele, where an invariant lysine in the Walker A box is mutated to alanine, which generates a helicase-dead allele (17). Mutant and WT proteins were epitope tagged at their carboxyl termini with three FLAG tags for detection by western blotting.

To determine if the SM is essential for ScPif1 functions, we deleted most of the SM (21 of the 23 amino acids). We also deleted six amino acids (Pro367 to Gln372) that form part of the extended loop (Figure 2C, group II). The first 10 amino acids of the SM form part of an α-helix (41–43). To test the importance of the α-helical portion of the SM, we replaced the first 15 residues (Asp352 to Gln366) with 15 alanines, as poly-alanine cannot form an α-helix, but still provides structural flexibility. To determine if the α-helical structure or simply the sequence of this region was important, we replaced the first 15 SM residues with the SM sequence from the bacterial *Bacteroides spp* Pif1 (BsPif1), which is different from that of the ScPif1 SM at 12 of the 15 positions (although four of the 12 changes are conservative) (Figure 2B). We also generated a more drastic mutant that replaced the 10 SM amino acids of the α-helix with a completely different sequence that is nonetheless predicted to form an α-helix by the SABLE protein structure prediction server (53). For this allele, we used the Lys123 to Ile132 amino acid region from the T4 bacteriophage Dda helicase (54). We chose the Dda sequence because using the Pymol program (55), it aligned well with the ScPif1 SM α-helix and is located in a similar position as the SM within the Dda protein; i.e. between helicase motifs II and III (Supplementary Figure S1). To test the significance of the SM loop in the carboxyl-terminal region, single alanine substitutions (Figure 2C, group I) or successive

amino acid substitutions (Figure 2C, group III) were created. Single amino acid substitutions were also created at specific sites within the SM, including a change that corresponds to the hPIF1-L319P mutation (*Sc-pif1*-L354P) that is associated with higher breast cancer risk (44) (Figure 2C, group I).The growth rates of cells expressing each *TRP1*-marked mutant allele were determined for cells growing at 30°C in media lacking tryptophan (Supplementary Figure S2B). Mutations that were functional in the *in vivo* assays described below had normal growth rates while cells with null or near null alleles grew more slowly, a phenotype that can be explained by their reduced mitochondrial function.

All of the SM alleles except *Sc-pif1-L354P* produced stable protein in yeast

After generating *pif1Δ* cells carrying a centromere plasmid borne copy of a mutant Sc*PIF1* allele, we used western blot analysis to determine if the mutant proteins were expressed *in vivo*. All of the ScPif1 SM mutants generated for this study were expressed, except for ScPif1-L354P, whose expression was not detectable by western blotting. Therefore, this mutant was not examined in functional assays. Quantification of the expression of key SM mutants indicated some variability in protein levels (Supplementary Figure S2A). However, changes in protein levels did not correlate with loss of ScPif1 function.

The SM is essential for the mitochondrial functions of ScPif1

ScPif1 is critical for the maintenance of mtDNA as loss of ScPif1 rapidly generates respiratory deficient cells (petites) (15). To test for mitochondrial proficiency we analyzed growth on glycerol, a non-fermentable carbon source. Petites are unable to grow with glycerol as the only carbon source. Plasmids carrying WT or mutant Sc*PIF1* alleles were transformed into a heterozygous diploid strain (YCG59, *pif1Δ*/WT), and tetrads were dissected. After spore clones grew up on glucose plates, which allowed for loss of mtDNA, *pif1Δ* cells carrying either WT or a mutant allele of Sc*PIF1* were spotted onto selective medium containing either glycerol or glucose. Growth was assessed after ∼3 days at 30°C (Figure 3). Cells expressing single alanine substitutions within the SM exhibited WT mitochondrial function as shown by robust growth on glycerol plates. However, deletion of the entire SM, deletion of the loop region and larger amino acid replacements did not generate respiratory proficient cells. Thus, the SM of ScPif1 is critical for maintenance of mtDNA.

The SM is critical for ScPif1 to remove telomerase from telomeres

ScPif1 catalytically removes telomerase from telomeres in a manner that limits telomere lengthening (18). Thus, compared to WT cells, cells lacking ScPif1 have long telomeres (16,18). We used Southern blot analysis to monitor telomere length in cells expressing each of the mutant alleles (Figure 4). Most of the single alanine substitutions exhibited telomere lengths similar to WT (Figure 4; lanes 1, 2, 7 and 8), indicating that subtle changes in the SM did not disrupt the ability of ScPif1 to regulate telomere length. Cells expressing alleles that deleted the entire SM, the loop region or more substantial amino acid substitutions resulted in long telomeres similar in length to telomeres in *pif1Δ* cells (Figure 4; lanes 3–6 and 15–18). However, three of the seven single alanine substitutions (G369A, G370A and Q372A) exhibited intermediate telomere phenotypes, suggesting that these residues are required for full inhibition of telomere elongation (Figure 4; lanes 9–14).

The SM is critical for ScPif1's role in Okazaki fragment processing

Deletion of *PIF1* suppresses the lethality caused by deletion of *DNA2*, an essential gene whose protein product has both helicase and nuclease activities (22,23). The basis for this suppression is that Pif1 is required to generate Okazaki fragments with long 5′ flaps whose resolution is Dna2-dependent. To assess the importance of the SM for ScPif1's role during Okazaki fragment processing, the viability of *pif1Δ dna2Δ* cells expressing a plasmid borne allele with a SM mutant was assessed (Figure 5). Seven mutants each with a single alanine substitution (e.g. L354A and P367A) failed to suppress the lethality of a *dna2Δ* mutant indicating that these alleles were able to generate long-flap Okazaki fragments. However, deletions and more substantial amino acid substitutions (e.g. successive alanine changes or α-helix sequence replacements) generated viable cells, indicating that the mutant ScPif1 suppressed the *dna2Δ* lethality. Therefore, the SM was essential for Pif1 function during Okazaki fragment processing. Replacement of the SM with the bacterial BsPif1 SM sequence also suppressed the *dna2Δ* lethality. Thus, as with telomere length regulation (Figure 4), the bacterial SM was unable to provide the Okazaki fragment processing activity of WT ScPif1, even though it did provide its mitochondrial function (Figure 3). Of the 15 SM mutants tested here, the bacterial SM substitution mutant (BsPif1-SM allele) was the only separation of function allele we obtained.

The SM is critical for ScPif1 to remove telomerase from double strand breaks

In addition to regulating the lengths of existing telomeres, Pif1 removes telomerase from DSBs, thus inhibiting *de novo* telomere addition (19). *De novo* telomere additions were detected by a GCR assay that selects for the simultaneous loss of two markers on the left arm of chromosome V (Figure 6A) (21). To determine if the SM affects *de novo* telomere addition, the rate at which GCR events occurred in strain MBY77 carrying plasmid borne WT or mutant alleles of Sc*PIF1* was calculated (Figure 6B). The GCR rate for cells expressing WT ScPif1 was 1.20×10^{-7} events per cell division. The rates for cells expressing *pif1*-P367A as well as those for the three alleles that had intermediate telomere lengths (*pif1*-G369A, G370A and Q372A) were similar to WT cells. In contrast, the GCR rates in cells expressing an allele lacking part of the SM (SMΔ6) or with multiple tandem alanine substitutions (SM6A) were almost 50-fold higher than in WT cells. Thus, the SM is also essential to inhibit *de novo* telomere additions.

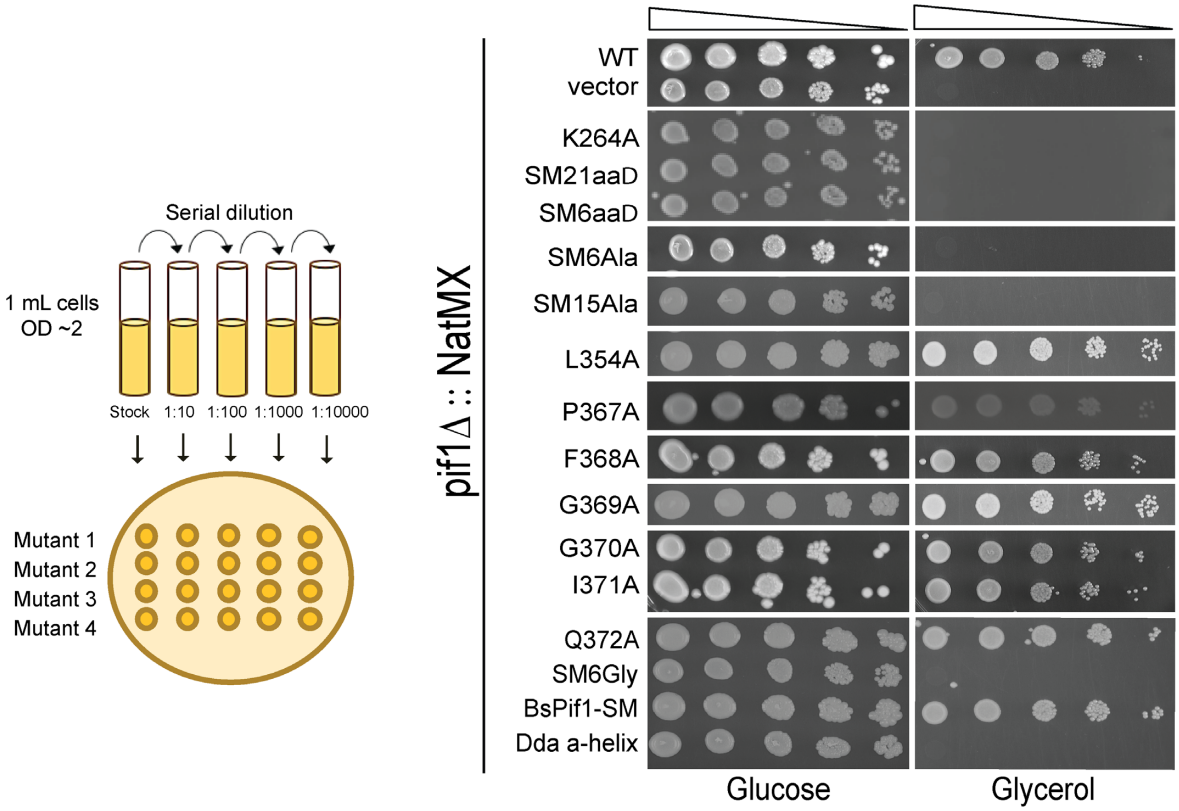

Figure 3. Analyzing ScPif1 SM mutants for mitochondrial proficiency. As indicated in the cartoon on the left of the figure, cultures were 10-fold serially diluted left-to-right and spotted on selective media containing glucose or glycerol. Respiratory deficient cells grow on media containing glucose but not on media containing glycerol.

The PFGGIQ region within the ScPif1 SM is required for ATPase activity

Analysis of the *in vivo* phenotypes of SM mutants (Table 1) indicated that while no single amino acid was required for function, the entire 23 amino acid region as well as subsets of the region were necessary. Within the 23 amino acid SM, deletion or substitution of the conserved ^{367}PFGGIQ^{372} motif was sufficient to lead to a null phenotype *in vivo* indistinguishable from that of *pif1Δ* or the *pif1-K264A* allele. This observation suggests that the change of this six amino acid stretch affects one or more of ScPif1's biochemical functions, e.g. DNA binding, the DNA-dependent ATPase activity or the ATPase-coupled unwinding activity. To distinguish among these possibilities, we purified ScPif1 variants containing selected SM mutations. Consistent with a WT phenotype *in vivo*, the ScPif1 constructs harboring the single-point mutations G370A or I371A retained DNA-dependent ATPase activity *in vitro*, the major catalytic activity that drives ScPif1 functions (Figure 7B). The differences in the DNA-dependent ATPase activity (both in the apparent K'_{DNA} and k'_{cat}; see table associated with Figure 7B) between WT ScPif1 and these single-point mutant variants did not result in dramatic differences in ScPif1 functions *in vivo* (Table 1). In contrast, the full-length ScPif1 variants harboring a deletion of the ^{367}PFGGIQ^{372} motif (SMΔ6) or a substitution of this region with six alanines (SM6A) did not show ssDNA-dependent ATPase activity, even at a 10-fold higher concentration of enzyme (Figure 7C). However, both variants co-purified with a contaminating band that could not be removed, even with size-exclusion chromatography (Figure 7A, asterisks). To test whether the loss of ATPase activity in these mutants was due to the presence of the contaminating band, we generated a substitution of the ^{367}PFGGIQ^{372} motif with six glycines (SM6G) within a Pif1 construct that lacked the N-terminal region of the helicase (Pif1$^{238\text{-}859}$-SM6G). The purified protein did not contain detectable amounts of the contaminating band (Figure 7A), yet, neither ssDNA nor a forked-DNA substrate (i.e. an unwinding substrate) stimulated ATPase activity, even at an enzyme concentration that was 10-fold higher than that of its WT counterpart (Figure 7D). However, the SM6G variant of ScPif1$^{238\text{-}859}$ retained DNA binding activity, as monitored by quenching of fluorescence intensity of a forked-DNA substrate labeled with 6-carboxyfluorescein (Figure 7E). Thus, loss of DNA-dependent ATPase activity in this mutant was not due to loss of DNA binding activity. Taken together, the *in vitro* results indicate that while large changes within the ^{367}PFGGIQ^{372} motif of the SM did not lead to loss of DNA binding activity of ScPif1, they eliminated its ATP binding and/or hydrolysis activities.

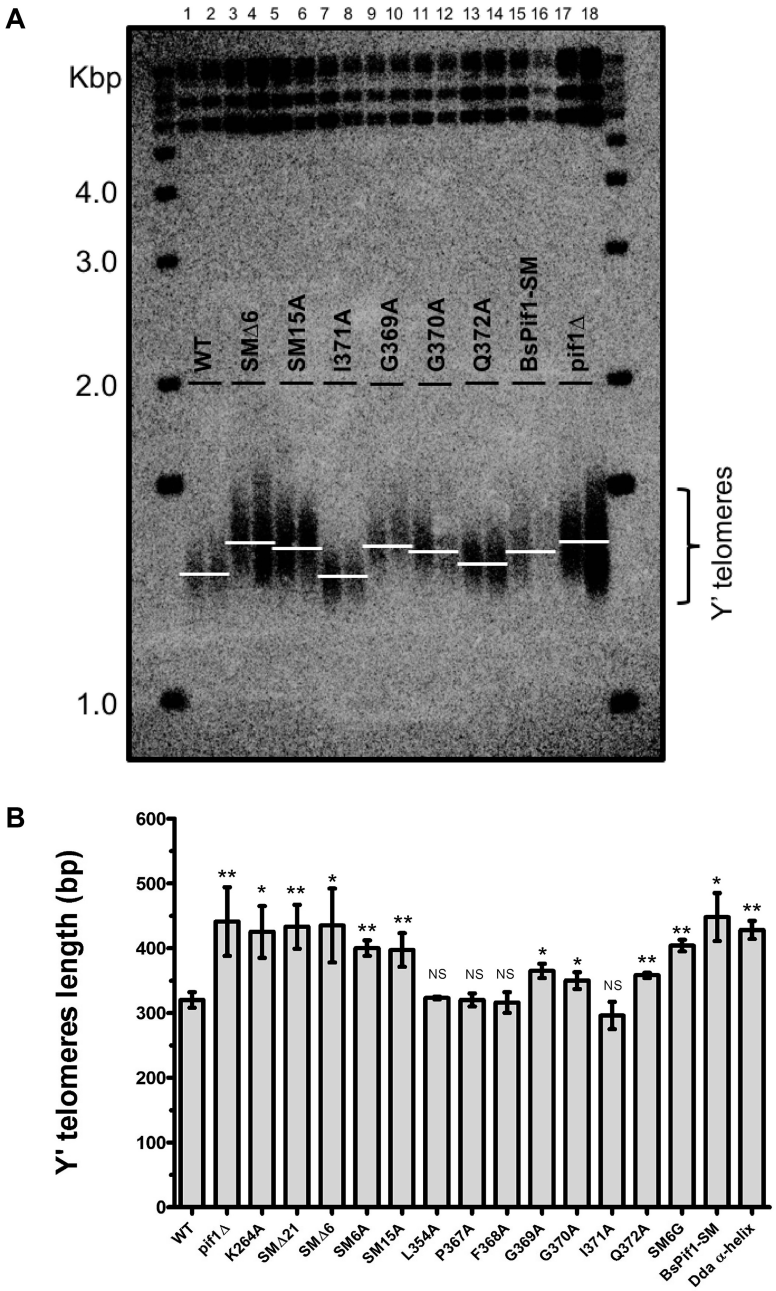

Figure 4. (**A**) Analysis of telomere lengths in cells expressing different *PIF1* alleles. Genomic DNA was isolated from three or more independent isolates from each of the 14 SM mutant strains as well as from WT, *pif1Δ* and catalytically dead *pif1*-K264A cells (in this figure two representative examples are shown for 9 of the 17 strains examined). DNA was digested with XhoI, separated on 1% agarose gels and analyzed by Southern hybridization using a radiolabeled sub-telomeric Y' probe (48). The lanes contain DNA from WT (lanes 1 and 2), SMΔ6 (lanes 3 and 4), SM15A (lanes 5 and 6), I371A (lanes 7 and 8), G369A (lanes 9 and 10), G370A (lanes 11 and 12), Q372A (lanes 13 and 14), BsPif1-SM (lanes 15–16) and *pif1Δ* (lanes 17 and 18). (**B**) Quantitation of telomere lengths. To obtain the number of base pairs of TG_{1-3} telomeric DNA, 875 bp, the amount of Y' DNA in the terminal XhoI restriction fragment (48) was subtracted from the size of the terminal fragments. The average telomere length was determined for at least three biological isolates per strain. The white lines represent the peak DNA signal that indicates the average length of the Y' telomeres. Telomeres were classified in Table 1 as having WT (320 ± 12 bp), intermediate (357 ± 11 bp) or null (441 ± 53 bp) telomere lengths. Error bars are standard deviations. Given that loss of ScPif1 function results in longer telomeres, a one-tailed student *t*-test was used to compare the mean telomere lengths between WT and ScPif1 mutants to determine if the increase in telomere lengths observed in the SM mutants was statistically significant; NS, not significant, $*P<0.05$, $**P<0.005$.

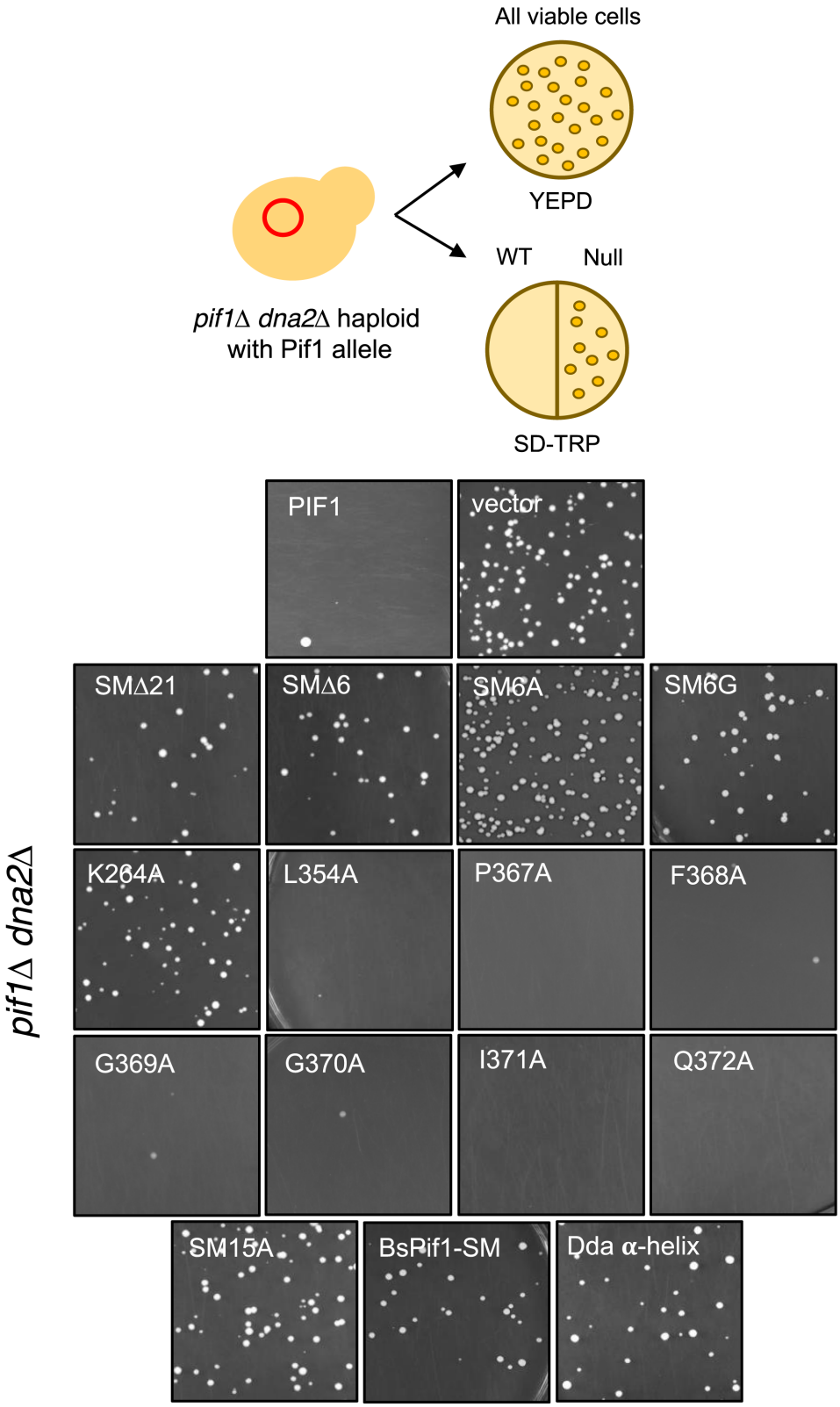

Figure 5. Analysis of the ability of ScPif1 SM mutants to suppress the lethality of a *dna2Δ* cells. Plasmid-borne WT and SM alleles were introduced into *pif1Δ dna2Δ* cells and analyzed for growth on selective media as indicated in the cartoon. WT alleles are unable to suppress the lethality of *dna2Δ* cells. Images shown are cells plated on selective media lacking tryptophan; growth indicates null ScPif1 function.

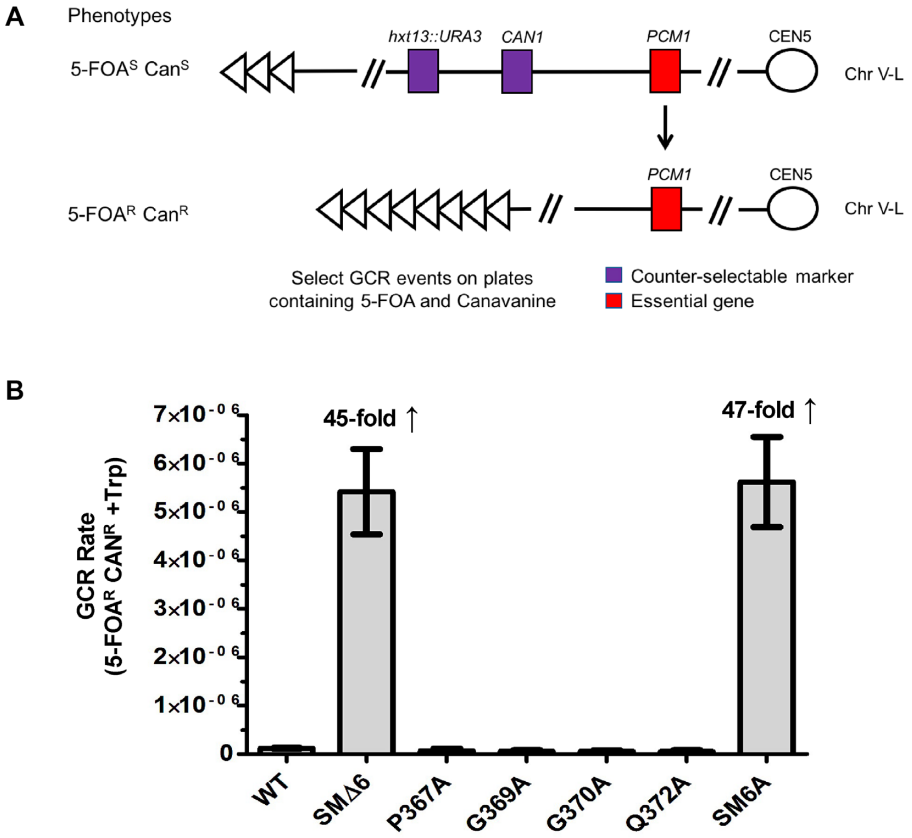

Figure 6. (**A**) Schematic of gross chromosomal rearrangement (GCR) assay (49). (**B**) Bar graph shows GCR rates of WT ScPif1, P367A, SMΔ6, G369A, G370A, Q372A and SM6A mutants. The average rate in cells expressing WT ScPif1 was 1.20×10^{-7} events per cell division and the average rates in mutant cells expressing single alanine substitutions were similarly low. The GCR rate for cells expressing P367A, an allele that was WT in all *in vivo* assays, was 6.68×10^{-8}. The GCR rate for cells expressing G369A, G370A and Q372A, alleles that exhibited an intermediate telomere phenotype, were 5.85×10^{-8}, 5.79×10^{-8} and 5.36×10^{-8}, respectively. In contrast, the average rates in mutant strains SMΔ6 and SM6A were almost 50-fold higher compared to WT. Experiments were done on at least three biological replicates. Error bars show standard deviations.

DISCUSSION

The SM is a unique feature of Pif1 family helicases, yet its importance for the diverse functions of these proteins was unknown. By making a series of mutations in the SM of ScPif1, we showed that the SM is critical for ATPase activity *in vitro* and for multiple *in vivo* functions of this multifunctional DNA helicase. These conclusions agree with and complement those in an accompanying paper that shows that the SM in the fission yeast Pfh1, another member of the Pif1 family of DNA helicases, is essential for all of its *in vitro* activities, except DNA annealing, including its preferential unwinding of G4 and RNA/DNA hybrids (see accompanying paper by Mohammad *et al.* (45)).

Previous studies have addressed the *in vitro* functions of the SM in bacterial helicases (41,42). Mutation of the equivalent amino acid identified in the cancer-variant of hPIF1 resulted in more than 90% reduction of ssDNA binding, double-stranded DNA (dsDNA) and G4-DNA unwinding activities of BaPif1 (42). Also, a deletion of the conserved four amino acids PFGG within the loop region of BsPif1 abolishes its unwinding activity (41). In our SM study, we tested mutations of almost all the residues within the SM for effects on ScPif1 functions *in vivo* as well as several of these mutations for their effects *in vitro*. Although substitution of an alanine residue at seven different highly conserved residues throughout the SM yielded active protein *in vivo* (and for two of these substitutions, *in vitro* as well), deletion of most of the 23 amino acid SM (SMΔ21) was as defective *in vivo* as a complete deletion of the *PIF1* gene or the catalytically dead K264A allele (Table 1). As the SMΔ21 allele produced a stable protein, its lack of *in vivo* function was not due to its producing an unstable product (Supplemental Figure S2A). Likewise, deletion of six amino acids near the carboxyl end of the SM (SMΔ6), one of the most highly conserved regions within the motif (Figure 2B), was a null allele *in vivo*, as was the SM6A and SM6G alleles where the same six amino acids were replaced with consecutive alanines or glycines. The null phenotypes of the SMΔ6 and SM6A alleles *in vivo* can be explained by our *in vitro* data showing their lack of ATPase activity, but not DNA binding. Thus, although single alanine substitutions at these positions were WT for several *in vivo* functions, their consecutive replacement generated non-functional protein. In the crystal structure, starting with the proline residue, which is proposed to create a kink, these six amino acids form part of an extended loop (41–43). Thus, not only the presence but also the sequence of this highly conserved six amino acid portion of the loop (^{367}PFGGIQ^{372}) were essen-

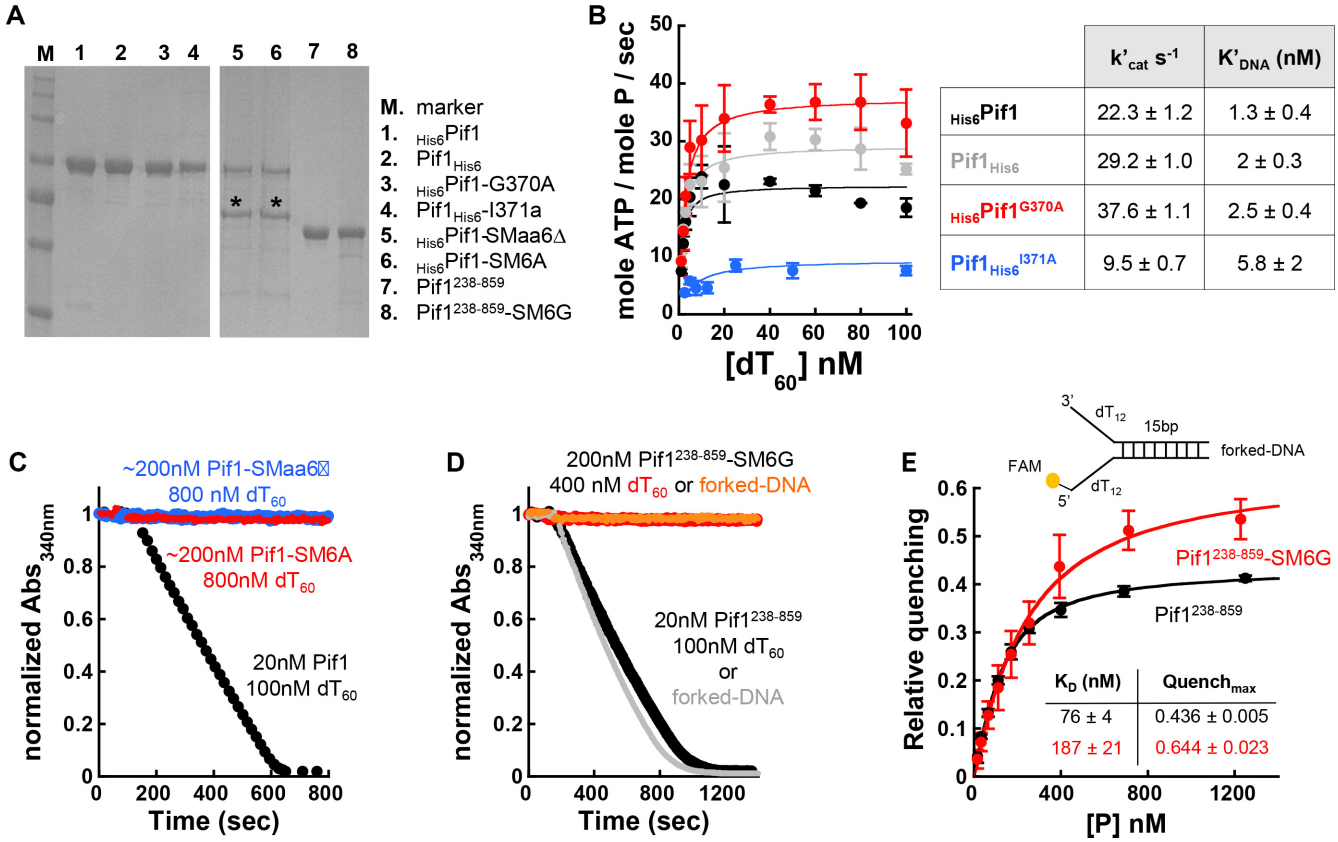

Figure 7. The SM of ScPif1 is required for DNA dependent ATPase activity *in vitro*. (**A**) SDS-PAGE analysis of the purified ScPif1 WT and mutant ScPif1 proteins prepared in *Escherichia coli*. The asterisk indicates a contaminating band that co-purifies with full-length Pif1 variants with mutations within the SM. (**B**) DNA-dependent ATPase activity of Pif1 (N- and C-terminal His_6-tagged) and the single-point mutant variants G370A and I371A. (**C**) Time course of ATP hydrolysis, monitoring the absorbance of NADH, of Pif1 and its SMaa6Δ and SM6A variants. (**D**) Time courses of ATP hydrolysis of $Pif1^{238-859}$ and its SM6G variant. (**E**) Forked-DNA binding activity of $Pif1^{238-859}$ and its SM6G variant.

tial for ScPif1 functions *in vivo*. The $Pif1^{238-859}$ SM6G protein bound a forked-DNA substrate *in vitro*, although its affinity was ∼2.5x lower than the WT ScPif1 (Figure 7E). Thus, the SM is not essential for substrate binding, but it may enhance binding as suggested in (42). The SM is situated between helicase motifs II (Walker B box) and III, and these canonical motifs are known to be involved in NTP hydrolysis and DNA binding, respectively (4). Given the SM's location, we speculate that the conserved loop region may provide the appropriate spatial configuration required for the residues from motifs II and III to coordinate and couple the energy of ATP binding/hydrolysis with DNA unwinding.

To test if the six highly conserved amino acids in the loop region are sufficient for SM function, we replaced the amino terminal 15 amino acids of the SM with fifteen alanines (SM15A). In all tested *in vivo* functions, SM15A was a null allele, even though it produced stable protein *in vivo*. Thus, the conserved six amino acid portion of the loop region was necessary but not sufficient for SM function. The amino terminal 10 amino acids are part of an α-helix (41–43). Given that SM15A was a null allele and contained a poly-alanine sequence that is unable to form an α-helix, these results suggest that the α-helical structure of this region was also critical for function. To determine if the presence of an α-helix plus the loop region were sufficient to supply SM activity, we replaced the 10 amino acid helix-forming region with 10 amino acids from the bacteriophage dda helicase (Dda α-helix), which is predicted to form an α-helix. We also replaced this region with the comparable part of the *Bacteriodes spp* Pif1 family helicase (BsPif1-SM), which also forms an α-helix (41,42), but whose sequence is fairly divergent from that of the equivalent region of ScPif1 (Figure 2B). Although expressed normally, both of these mutant proteins lacked all (Dda) or some (BsPif1-SM) of the *in vivo* functions of ScPif1 (Supplemental Figure S2A, Table 1) Therefore, not only the structure but also the sequences of the α-helix and the loop regions in the SM are essential for *in vivo* function.

ScPif1 and the *S. pombe* Pfh1 DNA helicases are multifunctional *in vivo* (see introduction and (56)). Unlike Rrm3 (57) or the *S. pombe* Pfh1 (58), ScPif1 does not move with the replisome but is probably recruited to its diverse targets during or after replication of the sequence (27) (Chen *et al.*, in preparation). A long standing interest in our lab is to identify regions of ScPif1 that might target it to its diverse *in vivo* substrates. However, with few exceptions, a given SM allele was either functional or non-functional for all tested *in vivo* functions. The exceptions include three of the single alanine substitutions (G369A, G370A and Q372A) in the

Table 1. Summary table showing effects of SM mutations on individual ScPif1 functions *in vivo*. **(A)** All the SM mutants were tested for effects on mitochondrial function, telomere length and Okazaki fragment processing. Telomeres were classified as having WT (320 ± 12 bp), intermediate (357 ± 11 bp) or null (441 ± 53 bp) telomere lengths. **(B)** A subset of the SM mutants exhibiting WT and partial loss of function phenotypes was further tested for effects on *de novo* telomere addition. The GCR rate for the SM mutants tested was classified as WT or null. Dash in Table 1A indicates that the GCR rate for that SM mutant was not determined

(A)

ScPif1 allele	Mitochondrial function	Telomere length	*De novo* telomere addition	Okazaki fragment processing
WT	WT	WT	WT	WT
pif1Δ	Null	Null	–	Null
K264A	Null	Null	–	Null
SM amino terminal mutants				
SMΔ21	Null	Null	–	Null
L354A	WT	WT	–	WT
SM15A	Null	Null	–	Null
BsPif1-SM	WT	Null	–	Null
Dda α-helix	Null	Null	–	Null
SM carboxyl terminal mutants				
SMΔ6	Null	Null	Null	Null
P367A	WT	WT	WT	WT
F368A	WT	WT	–	WT
G369A	WT	Intermediate	WT	WT
G370A	WT	Intermediate	WT	WT
I371A	WT	WT	–	WT
Q372A	WT	Intermediate	WT	WT
SM6A	Null	Null	Null	Null
SM6G	Null	Null	–	Null

(B)

ScPif1 allele	Average GCR Rate (5-FOA^R CAN^R + TRP)
WT	1.20×10^{-7}
SMΔ6	5.42×10^{-6}
P367A	6.68×10^{-8}
G369A	5.85×10^{-8}
G370A	5.79×10^{-8}
Q372A	5.36×10^{-8}
SM6A	5.62×10^{-6}

loop region of the SM. All three had intermediate telomere lengths, longer than WT cells but shorter than telomeres in *pif1Δ* cells (Figure 4). Small differences in average telomere lengths are probably easier to detect than similarly small differences in the other *in vivo* functions examined in this paper. However, of the 15 SM mutants, these three were the only ones to have intermediate effects on telomere length. By both *in vivo* and *in vitro* assays, ScPif1 uses its ATPase activity to remove telomerase from DNA ends, resulting in a less stable telomerase–telomeric DNA interaction and hence a less processive telomerase (18,19). In contrast, single-point mutations of residues G370 and I371 resulted in different effects on the ATPase activity *in vitro*, with I371A having a negative impact and G370A being slightly more active than WT ScPif1 (Figure 7). The molecular origin of these differences remain to be determined, as is the quantitative relationship between the degree of ATPase activity *in vitro* and telomere function *in vivo*. Because the DNA-dependent ATPase activity of Pif1-G370A was similar, if not slightly better, to that of the WT enzyme (Figure 7B), the defect in these telomere-specific partial loss of function alleles may be manifest only *in vivo*. For example, the intermediate telomere length phenotypes could be due to partial disruption of a protein–protein interaction that recruits ScPif1 to telomeres.

The BsPif1-SM allele is our best example of a separation of function allele. In this allele, the 15 amino acid stretch that forms part of the α-helix and the first part of the loop in the ScPif1 SM was replaced with the corresponding sequence from *Bacteroides spp* Pif1. The SM sequence in this allele also contains the six highly conserved amino acids in the loop region (^{367}PFGGIQ^{372}). The BsPif1-SM allele had WT mitochondrial function but was a null for three nuclear functions (Table 1). Because all tested nuclear functions were defective in this mutant, its phenotype is hard to explain by loss of a protein–protein interaction that targets ScPif1 to a specific substrate. However, loss of nuclear functions could be explained if the BsPif1-SM protein is deficient in nuclear localization. Translation of ScPif1 can begin at either the first or second methionine in the open reading frame (16,17). Between the first and second methionine is a mitochondrial localization signal. Thus, if translation begins at the first methionine, as it commonly does (59), the translated protein is targeted to mitochondria. If translation begins at the second methionine, the protein is targeted to nuclei. From its sequence, the ScPif1 SM is unlikely to encode a nuclear localization signal (NLS). However, the protein made by the BsPif1-SM allele might change the presentation of the as yet unidentified NLS, as in the crystal structures, the BsPif1 SM interacts with the 1B domain, which

folds into an unstructured loop (41), while the 1B domain of ScPif1 forms an α-helix (43).

In both ScPif1 (Figure 7) and the fission yeast Pfh1 (see accompanying paper by Mohammad *et al.*, (45)) the SM was not needed to bind to ssDNA and/or other DNA substrates *in vitro.* Moreover, the ScPif1 SM was not required for protein stability as ScPif1 and Pfh1 variants lacking almost the entire SM were stable *in vitro* (Figure 7) (see accompanying paper by Mohammad *et al.* (45)). Only one of the 15 ScPif1 SM mutants was unstable *in vivo*, ScPif1-L354P, the equivalent of the cancer-associated hPIF1 variant, hPIF1-L319P. In contrast, the equivalent *S. pombe* SpPfh1-L430P mutant was stable *in vivo* and *in vitro* but inactive for *in vivo* and *in vitro* ATP-dependent activities (44) (see accompanying paper by Mohammad *et al.* (45)). Similar to the *S. pombe* Pfh1, analysis of the equivalent *Bacteriodes spp* BaPif1 I118P mutant showed a significant reduction in ssDNA binding and dsDNA and G4-unwinding activities (42).

The analyses here and in the accompanying paper argue that the SM is essential for all functions that require the ATPase activity of Pif1 family DNA helicases. By extension, ScPif1 must act enzymatically for the tested *in vivo* functions. In contrast, the ability of ScPif1 (and Pfh1) to anneal complementary DNA strands does not require ATP hydrolysis (38,45). By using helicase dead alleles, such as *pif1*-K264A, all of the tested *in vivo* activities of ScPif1 are ATPase dependent [see, for examples (17,29,60), Chen *et al.*, in preparation]. Thus, as yet, there is no *in vivo* evidence for a function for ScPif1- (or Pfh1-) mediated strand annealing. However, the role of ScPif1 in fortifying the replication fork barrier in the rDNA (28), which has not been tested for ATPase-dependence, is a candidate for being mediated by strand annealing. Finally, if ScPif1 is recruited to its *in vivo* targets by specific protein–protein interactions, these interactions usually do not involve the SM region of ScPif1.

In summary, the combined data here and in the accompanying paper show that the SM regions of ScPif1 and fission yeast Pfh1 were essential for ATPase activity and for all tested *in vivo* functions but not for substrate binding or DNA annealing *in vitro*. Because we found little evidence for SM alleles that support only a subset of ScPif1's *in vivo* functions, sequences that define ScPif1 targeting to a specific genome region likely lie mainly outside the SM. The demonstration in the accompanying paper that Pfh1, like ScPif1 (34,38), has single strand annealing activity and preferentially unwinds RNA/DNA hybrids provides additional support that members of the Pif1 family of DNA helicases share not only sequence similarity but also common biochemical properties.

SUPPLEMENTARY DATA

Supplementary Data are available at NAR Online.

ACKNOWLEDGEMENTS

We thank Y. Kim for help with some of the experiments. We thank A. Tracyzk for useful discussions on protein structure, which helped us with the design of certain mutations and T. Pohl for helpful discussions.

FUNDING

National Institutes of Health (NIH) [1R35GM118279 to V.A.Z., 2R01GM098509 to R.G]; National Science Foundation [DGE1656466 to C.L.G.]. Funding for open access charge: NIH [1R35GM118279 to V.A.Z.].
Conflict of interest statement. None declared.

REFERENCES

1. Shiratori,A., Shibata,T., Arisawa,M., Hanaoka,F., Murakami,Y. and Eki,T. (1999) Systematic identification, classification, and characterization of the open reading frames which encode novel helicase-related proteins in Saccharomyces cerevisiae by gene disruption and Northern analysis. *Yeast*, **11**, 60–65.
2. Singleton,M.R., Dillingham,M.S. and Wigley,D.B. (2007) Structure and mechanism of helicases and nucleic acid translocases. *Annu. Rev. Biochem.*, **76**, 23–50.
3. Gorbalenya,A.E. and Koonin,E.V. (1993) Helicases: amino acid sequence comparisons and structure-function relationships. *Curr. Opin. Struct. Biol.*, **3**, 419–429.
4. Raney,K.D., Byrd,A.K. and Aarattuthodiyil,S. (2013) Structure and mechanism of SF1 DNA helicases. *Advances in Experimental Medicine and Biology*, **767**, 17–46.
5. Gorbalenya,A.E., Koonin,E.V., Donchenko,A.P. and Blinov,V.M. (1989) Two related superfamilies of putative helicases involved in replication, recombination, repair and expression of DNA and RNA genomes. *Nucleic Acids Res.*, **17**, 4713–4730.
6. Tuteja,N. and Tuteja,R. (2004) Unraveling DNA helicases Motif, structure, mechanism and function. *Eur. J. Biochem.*, **271**, 1849–1863.
7. Fairman-Williams,M.E., Guenther,U.P. and Jankowsky,E. (2010) SF1 and SF2 helicases: family matters. *Curr. Opin. Struct. Biol.*, **20**, 313–324.
8. Bochman,M.L., Sabouri,N. and Zakian,V.A. (2010) Unwinding the functions of the Pif1 family helicases. *DNA Repair*, **9**, 237–249.
9. Ivessa,A.S., Lenzmeier,B.A., Bessler,J.B., Goudsouzian,L.K., Schnakenberg,S.L. and Zakian,V.A. (2003) The saccharomyces cerevisiae helicase Rrm3p facilitates replication past nonhistone Protein-DNA complexes. *Mol. Cell*, **12**, 1525–1536.
10. Syed,S., Desler,C., Rasmussen,L.J. and Schmidt,K.H. (2016) A novel Rrm3 function in restricting DNA replication via an Orc5-Binding domain is genetically separable from Rrm3 function as an ATPase/Helicase in facilitating fork progression. *PLoS Genet.*, **12**, 1–28.
11. Muñoz-Galván,S., García-Rubio,M., Ortega,P., Ruiz,J.F., Jimeno,S., Pardo,B., Gómez-González,B. and Aguilera,A. (2017) A new role for Rrm3 in repair of replication-born DNA breakage by sister chromatid recombination. *PLoS Genet.*, **13**, 1–18.
12. Chung,W.-H. (2014) To peep into Pif1 helicase: multifaceted all the way from genome stability to repair-associated DNA synthesis. *J. Microbiol.*, **52**, 89–98.
13. Geronimo,C.L. and Zakian,V.A. (2016) Getting it done at the ends: Pif1 family DNA helicases and telomeres. *DNA Repair*, **44**, 151–158.
14. Foury,F. and Kolodynski,J. (1983) pif mutation blocks recombination between mitochondrial rho+ and rho- genomes having tandemly arrayed repeat units in Saccharomyces cerevisiae. *Proc. Natl. Acad. Sci. U.S.A.*, **80**, 5345–5349.
15. Lahaye,A., Stahl,H., Thines-Sempoux,D. and Foury,F. (1991) PIF1: a DNA helicase in yeast mitochondria. *EMBO J.*, **10**, 997–1007.
16. Schulz,V.P. and Zakian,V.A. (1994) The saccharomyces Pif1 DNA helicase inhibits telomere elongation and de novo telomere formation. *Cell*, **76**, 145–155.
17. Zhou,J.-Q., Monson,E.K., Teng,S.-C., Schulz,V.P. and Zakian,V.A. (2000) Pif1p helicase, a catalytic inhibitor of telomerase in Yeast. *Science*, **289**, 771–774.
18. Boulé,J.-B., Vega,L.R. and Zakian,V.A. (2005) The yeast Pif1p helicase removes telomerase from telomeric DNA. *Nature*, **438**, 57–61.
19. Phillips,J.A., Chan,A., Paeschke,K. and Zakian,V.A. (2015) The Pif1 helicase, a negative regulator of telomerase, acts preferentially at long telomeres. *PLOS Genet.*, **11**, e1005186.

20. Makovets,S. and Blackburn,E.H. (2009) DNA damage signalling prevents deleterious telomere addition at DNA breaks. *Nat. Cell Biol.*, **11**, 1383–1386.
21. Myung,K., Chen,C. and Kolodner,R.D. (2001) Multiple pathways cooperate in the suppression of genome instability in Saccharomyces cerevisiae. *Nature*, **411**, 1073–1076.
22. Budd,M.E., Reis,C.C., Smith,S., Campbell,J.L. and Myung,K. (2006) Evidence suggesting that Pif1 helicase functions in DNA replication with the Dna2 Helicase / Nuclease and DNA polymerase δ. *Mol. Cell. Biol*, **26**, 2490–2500.
23. Pike,J.E., Burgers,P.M.J., Campbell,J.L. and Bambara,R.A. (2009) Pif1 helicase lengthens some Okazaki fragment flaps necessitating Dna2 nuclease/helicase action in the two-nuclease processing pathway. *J. Biol. Chem.*, **284**, 25170–25180.
24. Tran,P.L.T., Pohl,T.J., Chen,C.-F., Chan,A., Pott,S. and Zakian,V.A. (2017) PIF1 family DNA helicases suppress R-loop mediated genome instability at tRNA genes. *Nat. Commun.*, **8**, 15025.
25. Osmundson,J.S., Kumar,J., Yeung,R. and Smith,D.J. (2016) Pif1-family helicases cooperatively suppress widespread replication-fork arrest at tRNA genes. *Nat. Struct. Mol. Biol.*, **24**, 162–170.
26. Ribeyre,C., Lopes,J., Boulé,J.-B.B., Piazza,A., Guédin,A., Zakian,V.A., Mergny,J.-L.L. and Nicolas,A. (2009) The yeast Pif1 helicase prevents genomic instability caused by G-quadruplex-forming CEB1 sequences in vivo. *PLoS Genet.*, **5**, e1000475.
27. Paeschke,K., Capra,J.A. and Zakian,V.A. (2011) DNA replication through G-quadruplex motifs is promoted by the Saccharomyces cerevisiae Pif1 DNA helicase. *Cell*, **145**, 678–691.
28. Ivessa,A.S., Zhou,J.Q. and Zakian,V.A. (2000) The Saccharomyces Pif1p DNA helicase and the highly related Rrm3p have opposite effects on replication fork progression in ribosomal DNA. *Cell*, **100**, 479–489.
29. Wilson,M.A., Kwon,Y., Xu,Y., Chung,W.-H., Chi,P., Niu,H., Mayle,R., Chen,X., Malkova,A., Sung,P. *et al.* (2013) Pif1 helicase and Polδ promote recombination-coupled DNA synthesis via bubble migration. *Nature*, **502**, 393–396.
30. Saini,N., Ramakrishnan,S., Elango,R., Ayyar,S., Zhang,Y., Deem,A., Ira,G., Haber,J.E., Lobachev,K.S. and Malkova,A. (2013) Migrating bubble during break-induced replication drives conservative DNA synthesis. *Nature*, **502**, 389–392.
31. Lahaye,A., Leterme,S. and Foury,F. (1993) PIF 1 DNA Helicase from Saccharomyces cerevisiae. Biochemical characterization of the enzyme. *J. Biol. Chem.*, **268**, 26155–26161.
32. Paeschke,K., Bochman,M.L., Garcia,P.D., Cejka,P., Friedman,K.L., Kowalczykowski,S.C. and Zakian,V.A. (2013) Pif1 family helicases suppress genome instability at G-quadruplex motifs. *Nature*, **497**, 458–462.
33. Zhou,R., Zhang,J., Bochman,M.L. and Zakian,V.A. (2014) Periodic DNA patrolling underlies diverse functions of Pif1 on R-loops and G-rich DNA. *eLife*, **3**, e02190.
34. Boulé,J.B. and Zakian,V.A. (2007) The yeast Pif1p DNA helicase preferentially unwinds RNA-DNA substrates. *Nucleic Acids Res.*, **35**, 5809–5818.
35. Chib,S., Byrd,A.K. and Raney,K.D. (2016) Yeast helicase Pif1 unwinds RNA:DNA hybrids with higher processivity than DNA:DNA duplexes. *J. Biol. Chem.*, **291**, 5889–5901.
36. Galletto,R. and Tomko,E.J. (2013) Translocation of Saccharomyces cerevisiae Pif1 helicase monomers on single-stranded DNA. *Nucleic Acids Res.*, **41**, 4613–4627.
37. Koc,K.N., Singh,S.P., Stodola,J.L., Burgers,P.M. and Galletto,R. (2016) Pif1 removes a Rap1-dependent barrier to the strand displacement activity of DNA polymerase δ. *Nucleic Acids Res.*, **44**, 3811–3819.
38. Ramanagoudr-Bhojappa,R., Byrd,A.K., Dahl,C. and Raney,K.D. (2014) Yeast Pif1 accelerates annealing of complementary DNA strands. *Biochemistry*, **53**, 7659–7669.
39. Zhang,D.H., Zhou,B., Huang,Y., Xu,L.X. and Zhou,J.Q. (2006) The human Pif1 helicase, a potential Escherichia coli RecD homologue, inhibits telomerase activity. *Nucleic Acids Res.*, **34**, 1393–1404.
40. Schmidt,K.H. and Kolodner,R.D. (2004) Requirement of Rrm3 helicase for repair of spontaneous DNA lesions in cells lacking Srs2 or Sgs1 helicase. *Mol. Cell. Biol.*, **24**, 3213–3226.
41. Chen,W.-F., Dai,Y.-X., Duan,X.-L., Liu,N.-N., Shi,W., Li,N., Li,M., Dou,S.-X., Dong,Y.-H., Rety,S. *et al.* (2016) Crystal structures of the BsPif1 helicase reveal that a major movement of the 2B SH3 domain is required for DNA unwinding. *Nucleic Acids Res.*, **44**, 2949–2961.
42. Zhou,X., Ren,W., Bharath,S.R., Tang,X., He,Y., Chen,C., Liu,Z., Li,D. and Song,H. (2016) Structural and functional insights into the unwinding mechanism of bacteroides sp Pif1. *Cell Rep.*, **14**, 2030–2039.
43. Lu,K.-Y., Chen,W.-F., Rety,S., Liu,N.-N., Wu,W.-Q., Dai,Y.-X., Li,D., Ma,H.-Y., Dou,S.-X. and Xi,X.-G. (2017) Insights into the structural and mechanistic basis of multifunctional S. cerevisiae Pif1p helicase. *Nucleic Acids Res.*, **46**, 1486–1500.
44. Chisholm,K.M., Aubert,S.D., Freese,K.P., Zakian,V.A., King,M.C. and Welcsh,P.L. (2012) A genomewide screen for suppressors of Alu-Mediated rearrangements reveals a role for PIF1. *PLoS One*, **7**, 1–10.
45. Mohammad,J.B., Wallgren,M. and Sabouri,N. (2018) The Pif1 signature motif of Pfh1 is necessary for both protein displacement and helicase unwinding activities, but is dispensable for strand-annealing activity. *Nucleic Acids Res.*, doi:10.1093/nar/gky654.
46. Gietz,R.D. and Schiestl,R.H. (2007) Quick and easy yeast transformation using the LiAc/SS carrier DNA/PEG method. *Nat. Protoc.*, **2**, 5–8.
47. Kushnirov,V.V. (2000) Rapid and reliable protein extraction from yeast. *Yeast*, **16**, 857–860.
48. Conrad,M.N., Wright,J.H., Wolf,A.J. and Zakian,V.A. (1990) RAP1 protein interacts with yeast telomeres in vivo: overproduction alters telomere structure and decreases chromosome stability. *Cell*, **63**, 739–750.
49. Putnam,C.D. and Kolodner,R.D. (2010) Determination of gross chromosomal rearrangement rates. *Cold Spring Harb. Protoc.*, **5**, 1–7.
50. Hall,B.M., Ma,C.-X., Liang,P. and Singh,K.K. (2009) Fluctuation analysis CalculatOR: a web tool for the determination of mutation rate using Luria-Delbruck fluctuation analysis. *Bioinformatics*, **25**, 1564–1565.
51. Singh,S.P., Koc,K.N., Stodola,J.L. and Galletto,R. (2016) A monomer of Pif1 unwinds Double-Stranded DNA and it is regulated by the nature of the Non-translocating strand at the 3′-End. *J. Mol. Biol.*, **428**, 1053–1067.
52. Barranco-Medina,S. and Galletto,R. (2010) DNA binding induces dimerization of saccharomyces cerevisiae Pif1. *Biochemistry*, **49**, 8445–8454.
53. Adamczak,R., Porollo,A. and Meller,J. (2005) Combining prediction of secondary structure and solvent accessibility in proteins. *Proteins Struct. Funct. Genet.*, **59**, 467–475.
54. He,X., Byrd,A.K., Yun,M.-K., Pemble,C.W., Harrison,D., Yeruva,L., Dahl,C., Kreuzer,K.N., Raney,K.D. and White,S.W. (2012) The T4 phage SF1B helicase Dda is structurally optimized to perform DNA strand separation. *Structure*, **20**, 1189–1200.
55. The PyMOL Molecular Graphics System, Version 2.0 Schrödinger, LLC.
56. Sabouri,N. (2017) The functions of the multi-tasking Pfh1Pif1 helicase. *Curr. Genet.*, **63**, 621–626.
57. Azvolinsky,A., Dunaway,S., Torres,J.Z., Bessler,J.B. and Zakian,V.A. (2006) The S. cerevisiae Rrm3p DNA helicase moves with the replication forkand affects replication of allyeast chromosomes. *Genes Dev.*, **20**, 3104–3116.
58. McDonald,K.R., Guise,A.J., Pourbozorgi-Langroudi,P., Cristea,I.M., Zakian,V.A., Capra,J.A. and Sabouri,N. (2016) Pfh1 is an accessory replicative helicase that interacts with the replisome to facilitate fork progression and preserve genome integrity. *PLoS Genet.*, **12**, e1006238.
59. Kozak,M. (1978) How do eukaryotic ribosomes select imitation regions in messenger RNA? *Cell*, **15**, 1109–1123.
60. Pike,J.E., Henry,R.A., Burgers,P.M.J., Campbell,J.L. and Bambara,R.A. (2010) An alternative pathway for okazaki fragment processing. *J. Biol. Chem.*, **285**, 41712–41723.